Photoconductive transients and one-dimensional charge carrier dynamics in discotic liquid crystals

A. Pecchia,* O. R. Lozman,* B. Movaghar,*,† N. Boden,* and R. J. Bushby*
Centre for Self-Organising Molecular Systems (SOMS), The University of Leeds, Woodhouse Lane, Leeds, LS2 9JT, United Kingdom

K. J. Donovan and T. Kreouzis‡
Department of Physics, Queen Mary, University of London, Mile End Road, London, E1-4NS, United Kingdom
(Received 29 August 2001; revised manuscript received 9 November 2001; published 26 February 2002)

Carrier transits and photoconductivity in hexaalkoxytriphenylene- (HAT) based liquid crystals and their binary 1:1 mixtures with hexaalkylphenyltriphenylene (PTP) are analyzed using time-dependent diffusion theory. The HAT6 derivatives, which show the best transits, can be modeled with a homogeneously distributed single-trap model. The transit data for the compound formed by the 1:1 binary mixture of HAT11-PTP9, which exhibits better columnar stability and higher carrier mobility, cannot, however, be explained using homogeneous multiple trapping models alone. The evidence presented in this paper also suggests that the trap-limited carrier relaxation does indeed obey the law of one-dimensional transport, which says that with an electric field, i.e., in the drift-limited regime, carriers take less time to reach the equilibrium values of the diffusivity. This is a particularly exciting result, which directly confirms rigorous theoretical predictions and is consistent with the previously discussed data taken in the crystalline phase of HAT6.

DOI: 10.1103/PhysRevB.65.104204 PACS number(s): 61.30.−v, 72.40.+w

I. INTRODUCTION

Disk-shaped molecules with rigid aromatic cores and flexible peripheral side chains can self-organize into structures that exhibit columnar order and liquidlike dynamics.[1] The columnar order is particularly pronounced in the readily synthesized hexalkoxytriphenylenes (HATn) (Fig. 1).[2] In time-of-flight (TOF) photoconduction experiments, HATn materials display well-defined, almost Gaussian, transits in the columnar liquid-crystalline (Col_h) phase. Such high-quality carrier transits in the dynamically disordered liquid-crystal (LC) phase are truly remarkable. In the solid phase the material is polycrystalline and the grain boundaries act as deep traps that produce strongly dispersive signals and no transits. In the isotropic phase, the magnitude of the photocurrent signal is small and difficult to detect. Depending on the sign of the applied field, either electron or hole transport can be observed.[3–6] Due to rapid trapping of electrons by oxygen and impurities no electron transport is observed in our experiments and this paper is therefore restricted exclusively to the interpretation of hole transport. The mobility of holes is found to be weakly temperature dependent and also essentially independent on electric field. It is interesting to note that the weak temperature dependence of the mobility is a feature common to many ordered organic solids that exhibit a TOF transit.[7] The systems under investigation are ''dynamically ordered'' columnar liquid crystals that, to some extent, can also be considered to be wide band-gap narrow-band semiconductors. It is generally agreed that conduction along the columns takes place by stochastic diffusion with varying degrees of quantum coherence, depending on the material under investigation and its phase. The exact nature of the temperature and field dependencies, however, is not completely understood and is still the subject of debate in the literature. We will discuss the current models in more detail in Sec. III. Charge-carrier mobilities can also be measured using pulse radiolysis time-resolved microwave conductivity (PR-TRMC) at 5 GHz. Both the time-of-flight experiment and the PR-TRMC give what is essentially a temperature-independent mobility in the LC phase. Pulse radiolysis can be thought of as the ''best'' or molecule-to-molecule value and it is possible to extract mobilities in temperature ranges where no transits are observed by TOF photoconduction. It is generally found that the mobility is discontinuous at the crystalline, liquid-crystalline, and isotropic boundaries and decreases at each phase boundary, respectively.

Conduction in triphenylene-based columnar liquid crystals is highly anisotropic; the charges move preferentially along the conducting aromatic cores of the columns with occasional intercolumnar hops through the insulating side-chain region. The motion perpendicular to the columns of recombining pairs has been analyzed in great detail in the works of the Warman group in Delft.[9] The anisotropy of the conductivity in doped HAT6 is $\sigma_{\parallel}/\sigma_{\perp} \sim 10^3$ and that in undoped HAT6 is $>10^4$.[8,9] Given the value of the mobility along the columns, $\mu_{\parallel} \sim 10^{-4}$ cm^2 V^{-1} s^{-1}, and given that the intra- and intercolumnar separations $a_{\parallel}$ and $a_{\perp}$ are of the orders of 3.5 and 19.5 Å in HAT6 (Fig. 2),[10,11] it is possible to estimate the degree of sideways diffusion in a typical transit time of 0.1 ms to be ~ 0.1 μm.[9]

We have shown in recent publications that the applicable properties of the triphenylene-based discogens can be improved by adding a stoichiometric amount of a substituted phenyltriphenylene (PTP) (such as PTP9, Fig. 1).[12–14] The resulting compounds, stabilized by dispersed quadrupolar and van der Waals interactions, form more ordered columnar mesophases, which are stable over a greater temperature range than the HAT or PTP components in isolation.[15] Evidence from x-ray-diffraction experiments and detailed molecular modeling studies suggest that the molecules of HAT and PTP alternate within the columns (Fig. 1).[12,14,16] The strength of the complimentary polytopic interaction (CPI)—the sum of dispersed quadrupolar and van der Waals forces

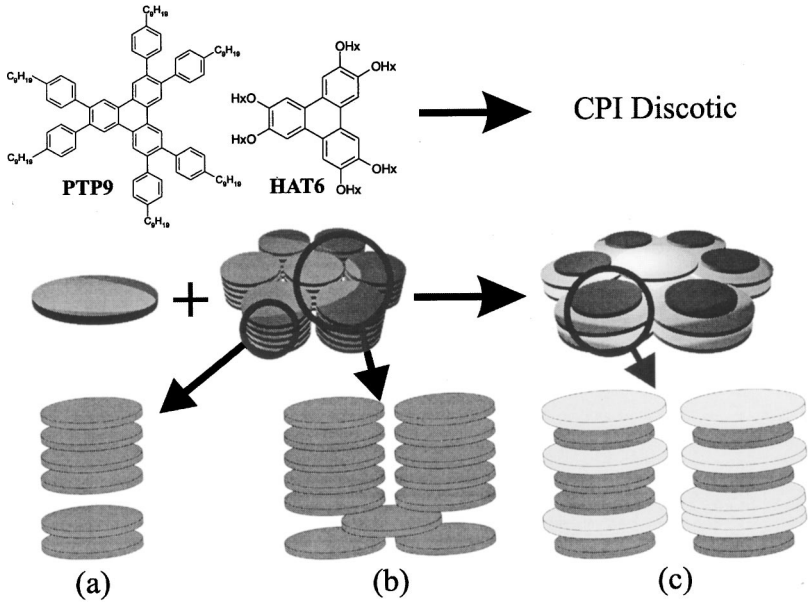

FIG. 1. Top shows the molecular structures of HAT6 and PTP9. When mixed in a 1:1 molar ratio the CPI stabilized compound is formed (illustrated in the center of figure). The HAT6 and PTP9 molecules are thought to alternate within the columns in an ABAB arrangement. The lower part of the figure illustrates the three main types of disorder in these systems. (a) shows the small amplitude intracolumnar fluctuation (weak and fast, included in the base diffusivity D_0), (b) shows the higher amplitude intercolumnar fluctuations (strong and slow, included as a trap term in the diffusion model), and (c) shows the additional type of disorder associated with AA or BB defects within the ABAB stacks of HAT6 and PTP9. Types (a) and (b) are expected for all Col_h phases while type (c) disorder is only expected in the specific case of the CPI stabilized discotics.

over all sites of inter- and intramolecular contact—determines the stability of the mesophase and the extent to which the clearing point of the 1:1 compound exceeds that of the individual components.[12,14] The charge-carrier mobilities in the CPI stabilized discotic mixtures are at least two orders-of-magnitude higher than those measured in the single-component HAT*n* systems and are comparable to that measured in the helical (*H*) phase of *HHTT*.[4,17] The mixed compounds have a solid phase that is glassy in nature; similar phases are also found to occur in HAT5 dimers.[18] In these materials TOF measurements are possible over a very broad range of temperatures because the glassy phase is reasonably homogeneous and does not have grain boundaries. In the LC phase, which extends between 65 °C and 165 °C, the mobility is found to be again very weakly temperature dependent.

The high-quality and almost one-dimensional properties of the transits, together with the relatively high mobilities, have motivated researchers to look for possible xerographic applications. The commercial applicability of these materials has been investigated in monomer and polymerized forms. In this context reproducibility is clearly an important issue. Photodegradation does occur in the isotropic phase and it can be detected in fluorescence decays as new exciton traps are generated.[19] In photoconduction applications, in the LC phase, the material is more stable and the TOF transients are reproducible to within a few percent of each other. In order to avoid memory effects associated with space charge and electric double layer formation the pulse energy has to be kept low and the sample is homeotropically aligned and annealed using a well-defined temperature cycling designed for optimal columnar alignment.

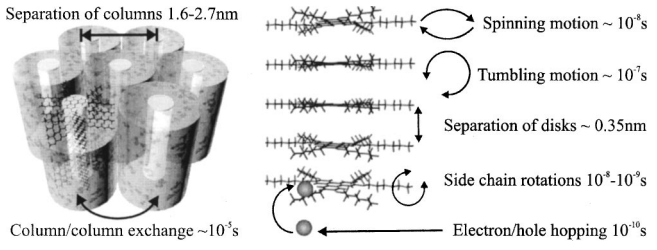

FIG. 2. Summarizes the dynamic nature of the Col_h phase. The left side shows a representation of the Col_h phase, the paradigm of a two-dimensional array of molecular wires. The right shows a close-up view of a single column. The distance measurements were reported in Ref. 10 (for HATn) and Ref. 11 (for the CPI compound HAT6+PTP9), and the dynamics in Ref. 9.

The observation of a transit and the knowledge that the materials are highly anisotropic is, on their own, insufficient proof that the transport is truly one dimensional; this must be demonstrated explicitly. For example, one-dimensional deep-trap-limited recombination obeys some very special time dependencies that have been evaluated by exact analytical methods.[20] The same applies to the time dependence of the diffusion coefficient when this is caused by disorder effects. It has been shown that even a small electric field can strongly influence the way the particle reaches its equilibrium value of diffusivity. These features are peculiar to one-dimensional dynamics. In one-dimensional random walks, the number of new sites visited grows with time as "$t^{1/2}$," but under the influence of an applied field F it grows as "eFt." This implies that the carrier reaches its equilibrium long-time dynamic value much more effectively than when the carrier is solely undergoing diffusion. In recombination, the effect of the field is to change the time dependence of the survival fraction from a stretched exponential law $[\exp-(t/t_0)^{1/3}]$ to a simple drift-limited exponential law. This behavior has been verified by the study of decay kinetics of charge carriers in the crystalline phase of HAT*n* materials.[6] The deep-trap formula with no release, though mathematically exact, gives a less perfect fit to the data than the model used by Donovan *et al.*,[21] which assumes that the trap is "shallow" and can release the carriers. Evidence that the system is one dimensional comes from the fact that the effective configurationally averaged trap rate scales with the inverse average time needed to reach a trap.[20]

When there is a clearly defined transit (as is the case in

the Col_h phase of HATn) it is also possible to see features characteristic of one-dimensional transport. Since a form of trapping, however shallow, is always present, the diffusivity is time dependent at short times. The drift motion has the effect of accelerating the equilibration process towards the steady-state diffusivity, because it takes less time for a carrier to reach the ''worst obstacle'' on its path to the counterelectrode.[22,23] The time-dependent diffusivity, $D(t)$, is expected to scale, for most trap distributions, as $D(t\eta)$, where η is the bias parameter $eFa/2kT$.[20] In this paper we verify this prediction in the Col_h phase of HAT6 by using a homogeneously distributed single-trap model. We also show that for the 1:1 HAT PTP compound, the problem is more complicated and needs at least two traps to give reasonable fits to the transits.

II. PHOTOCONDUCTIVE TRANSITS: THE INFLUENCE OF AN ABSORBING BOUNDARY

Consider a transient mobility experiment. If $I(t)$ is defined as the photocurrent produced by a light pulse at time $t=0$ then

$$I(t)=nfeFD(t)/kT, \tag{1}$$

where nf is the number of free carriers produced by the pulse and F is the applied bias field. Assuming that a percentage of photons is absorbed, generating excited electron-hole states, then the number of free carriers (nf) generated by the dissociation of these excitonic pairs is

$$nf=\eta I_L\Phi, \tag{2}$$

where ηI_L denotes the fraction of photons that have created excitons and Φ the probability that the charged pairs separate to form free carriers. This quantity is normally field and temperature dependent.

In the experimental wavelength regime of 337 nm, the nonscattered light is absorbed by molecular excitations from the $S0$ to the $S3$ states within about 0.1 μm.[24] The amount of light scattering depends on the physical state of the material, with the crystalline phase giving the largest scattering because of grain boundaries. The Onsager probability function (Φ) has exact analytic solutions in one dimension.[25] Photodissociation by the Onsager mechanism is, however, not the only way free carriers can be generated in this type of narrow-band, strongly excitonic, medium. For low fields and temperatures, the generation process can be due to the formation of molecular excitons, which diffuse to the metal interface where they can dissociate into free carriers more readily than in the bulk.[26]

The Onsager mechanism predicts that the peak photocurrent should initially vary as F^2 in one-dimensional systems. This is apparently not observed in HAT6.[27] The problem of charge generation in these materials appears to be subtle and more complex. Temperature dependence and dimensionality effects do not behave as predicted by Onsager's model in one dimension.[18] This problem needs a more detailed and focused treatment that goes beyond the scope of this paper (a paper is in preparation and will be published soon[27]).

As pointed out before, the diffusivity is given by $D(t)$, which is in general a time-dependent function because the liquid-crystal phase is ''disordered.'' However, the disorder in this case is dynamic; it is caused by the molecules moving in and out of the columns both along and perpendicular to the columnar axis (Fig. 2). Since we are dealing with a liquid crystal, the fluctuations create defects that then self-repair again on a time scale varying from 10^{-9} to 10^{-5} s.[10] Nevertheless at any instant (in the liquid-crystalline phase) the columns are indeed disordered, with displacements that are much larger than typical low-temperature harmonic phonon amplitudes. For our purposes, we can distinguish two possible classes of fluctuations. There are fluctuations small in amplitude [0.1–0.2 nm, Fig. 1(a)] but fast, so that their effect on the conduction process is limited to short times. The effect is an overall lowering of the overlap squared (or hopping probability) of up to an order-of-magnitude relative to the ''perfect case.'' The theory of transport with uniform ''small'' fluctuations is well described using the methods and results given in Ref. 28 and recovered below in Eq. (12) using an alternative derivation. The resistive processes associated with small fluctuations give a frequency-dependent response in a high-frequency range, inaccessible to our present experimental techniques. We shall therefore assume that the liquid like (small amplitude) columnar fluctuations simply lower the diffusivity to a constant value, called D_0. The second and larger amplitude fluctuations are associated with molecules jumping in and out of columns [Fig. 1(b)], where they constitute what is, in effect, a trap with a long delay time. These fluctuations can be treated explicitly in the framework of a trap and release model.[29] The experimental transit data will be used to estimate the trap delay times.[30] In order to fit and discuss transit curves, we introduce an absorbing boundary at L that simulates the absorbing electrode (and any associated double layer), and using the derivation given in Refs. 5, 6, and 31, we arrive at the following form for the Laplace transformed photocurrent:

$$I_p(p)=\int_0^\infty e^{-pt}I_p(t)dt, \tag{3}$$

$$I(p)=[eFn_f/kT][D(p)/p] \times[1-\exp\{-Np/[p+2\eta D(p)/a^2]\}], \tag{4}$$

where a is the intermolecular distance and $N=L/a$ is the number of molecular sites within the boundaries. The quantity $D(p)$ is the Laplace transform of $D(t)$, the trap-limited time-dependent diffusivity. The quantity $D(p)$ can be written generally as[32]

$$D(p)=pD_0/[p+\Sigma(p)], \tag{5}$$

where D_0 is the constant base diffusivity of the system and $\Sigma(p)$ is an effective delay function that depends on the trap distribution. The steady-state—short-time—diffusivity can be written in terms of an effective intermolecular hop rate, W:

$$D_0=a^2W. \tag{6}$$

The factor η in Eq. (4) is related, instead, to the bias field

$$2\eta = \frac{eF}{kT} a_{\parallel} \tag{7}$$

so that a hop to the right or left is given by $W(1+ \text{ or } -\eta)$, respectively.

III. THE ORIGIN OF D_0

In the relatively highly ordered Col_h phase of HATn, we can expect bandlike motion with short mean free paths along the columns, and long-range tunneling motion perpendicular to the columns. The resonance energy t_{ij} along the columnar stacks can be written in the form

$$t = t_0 e^{-\alpha|\mathbf{R}_i - \mathbf{R}_j|} \tag{8}$$

with $\alpha^{-1} \sim 2$ Å and $t_0 \sim 1.0$ eV. These values correspond to those of a charged molecule and the vectors $\mathbf{R}_i$ and $\mathbf{R}_j$ refer to the centers of the molecular cores. When the molecules are tilted with respect to each other, more than one variable is needed to describe the overlap energy.[20] The key quantity is the distance of closest approach between the π orbitals. In the present temperature range (300–400 K) and for present purposes, it suffices to use the approximate overlap integral given in Eq. (8).

The quantum diffusivity along the columns with small rapidly fluctuating disorder can be estimated using the Kubo-Greenwood formula to be of the form

$$D_{\alpha} = h/2\pi \Sigma_{\beta} |\langle \alpha | v_x | \beta \rangle|^2 \delta(E_{\alpha} - E_{\beta}). \tag{9}$$

Substitution of the velocity operator from the tight-binding model gives in the random-phase model[28]

$$D_0 = (2\pi/h) a^2 \langle t^2 \rangle \Delta \{ \langle E^2_{\text{homo}} \rangle + \langle \delta t^2 \rangle + \Delta^2 \}^{-1}, \tag{10}$$

where t is the resonance energy between two localized orbitals, $\langle E^2_{\text{homo}} \rangle$ is the mean squared of the energy spread of the homolevel induced by disorder, δt the amplitude of bandwidth fluctuations, and Δ is the width or energy uncertainty caused by fluctuations. Equation (10) is similar to the result derived in the framework of the Haken-Strobl-Reineker (HRS) model [see Eq. (4) in Ref. 28]. The HRS result is recovered if one assumes that the ''linewidth'' that drives the conduction process is also the width that causes the disorder broadening itself. If one uses

$$\Delta \sim \{ \langle E^2_{\text{homo}} \rangle + \langle \delta t^2 \rangle \}^{1/2}, \tag{11}$$

and substitutes Eqs. (11) into (10) one essentially recovers the same result as in Ref. 28 using the HRS model, which is given by

$$D_0 = a^2 \langle t^2 \rangle / 2 \{ \langle E^2_{\text{homo}} \rangle + \langle \delta t^2 \rangle \}^{1/2}. \tag{12}$$

The combination of Eqs. (10) and (12) describes the situation in which the fluctuations are fast on the time scale of structural trapping, but slow compared to t/h. The authors of Ref. 28 call this result the coherent process. In this limit, the fluctuations cause scattering and lower the diffusivity.

In the other extreme limit of strong disorder and localization, the diffusivity is dominated by the incoherent processes. In this case it is possible to derive a fluctuation-assisted diffusivity on the assumption that two neighboring localized states are orthogonal to each other until the orthogonality is lifted by bandwidth fluctuations. These then generate hopping transitions between equivalent orbitals with roughly the same energy to within kT. The diffusivity can then be written as

$$D_1 \sim 2\pi a^2 \langle (\delta t)^2 \rangle \tau_c / h, \tag{13}$$

where δt are the bandwidth fluctuations and τ_c is the correlation time of the fluctuating field. For fast fluctuations, τ_c is determined by the level broadening (the more general case is also considered by the authors of Ref. 28). The incoherent process takes over in the limit of very narrow bands, or at very low temperatures when the eigenstates are localized and orthogonal to each other.

The limit considered so far assumes that the coupling to the phonons is weak and can be treated in perturbation theory. Molecular calculations, however, show that polaronic relaxation energies of extra charges can be as much as 0.25 eV. Kreouzis *et al.*[33] have suggested that transport in discotic liquid crystals should be interpreted using polaronic hopping. They have fitted the temperature-dependent mobilities found in HAT6, HAT11, HAT6/PTP9, and HAT11/PTP9 to Holstein's small polaron jump rate in the high-temperature limit.[34] The extracted polaron binding energies and interpretations of the temperature-dependent mobility behavior are discussed in detail in Ref. 30.

The reader should note that in all three models, in order to obtain a temperature-independent behavior of the mobility, it is necessary to invoke a delicate balance of compensating processes in the formulas for the mobility. The authors of Ref. 28 apply the incoherent mechanism in a more generalized version of Eq. (13). They argue that the fluctuations in δt^2 due to librational and rotational degrees of freedom approximately compensate each other to give a temperature-independent mobility over a broad range of temperatures. In the polaron hopping mechanism, proposed in Ref. 33, it is the delicate balance between the temperature dependence of the exponential term and of the prefactor that gives rise to a temperature-independent mobility [$\exp(-E_p/kT)$, with E_p the polaron binding energy prefactor $\sim 1/T^{3/2}$].

An interesting model that gives rise to a temperature-independent mobility was obtained by Sumi.[35] In Sumi's model the coupling with the phonons gives rise to a phonon-assisted diffusivity that is proportional to the phonon occupation number. For energy differences smaller than kT the phonon modes are fully populated and the diffusivity is simply proportional to T. Hence, via the Einstein relation, the mobility becomes independent of temperature.

In this context it is important to mention the comprehensive Monte Carlo simulations applied to HAT5 dimers performed by van de Craats *et al.*[18] A temperature-independent mobility was obtained in the LC phase with a simple distribution of activated over-the-barrier hopping mechanisms. The effect of the distribution, in this case, is to make the

diffusivity essentially proportional to temperature and therefore the mobility temperature independent.

However, the measured magnitude of the mobilities in the discotic phase suggests that in the LC phase the magnitude of the effective hop rate can be as high as 10^{12} Hz, much faster than any of the structural or rotational modes. The carriers must be coherent over a mean free path bigger than the lattice constant. It seems therefore that the coherent formula given by Eq. (12) should be applicable to the evaluation of D_0. Looking at Eq. (12) the diffusivity is at best temperature independent, therefore the mobility scales as $1/kT$. The crossover between coherent and incoherent diffusion, and the discrimination between the various models requires further investigations.

IV. TRAPPING

Let us now consider the strong, more inhomogeneous fluctuation processes, which cause serious long-time delays. Following Ref. 29, we write a set of equations for the survival fraction of charge carriers ρ_f and the fraction of charges ρ_i, that are trapped in the type of trap i, homogeneously distributed in the sample:

$$\frac{\partial}{\partial t}\rho(x,t)=g(x,t)-\mu_0 F\frac{\partial}{\partial t}\rho_f(x,t)+D_0\frac{\partial^2}{\partial x^2}\rho_f(x,t), \tag{14a}$$

$$\rho(x,t)=\rho_f(x,t)+\sum_i \rho_i(x,t), \tag{14b}$$

$$\frac{\partial}{\partial t}\rho(x,t)=w_i\rho_f(x,t)-r_i\rho_i(x,t). \tag{14c}$$

In contrast to Ref. 29, however, we have kept the diffusion term in the solution for the free charges with diffusivity D_0. The quantity $g(x,t)=n_f\delta(x)\delta(t)$ is the generation function, consistent with the assumption that a planar sheet of charges is generated at time $t=0$ at position $x=0$. The system of Eqs. (14) can be solved by mean of a Laplace-Fourier transform technique. The current is calculated as the mean charge-carrier flux between the adsorbing boundaries with velocity $\mu_0 F$:

$$I(p)=en_f\mu_0 F\frac{1}{L}\int_0^L \rho_f(x,p)dx=en_f\mu_0 F\frac{1-\exp[-\gamma q(p)]}{\gamma q(p)[q(p)+1]} \tag{15}$$

with

$$q(p)=\sqrt{1+\frac{p}{\gamma^2 D(p)}}-1,\quad \frac{D(p)}{p}=\frac{D_0}{\left(p+\sum_i \frac{pw_i}{p+r_i}\right)},$$

$$\gamma=eFL/2kT(=\eta L^2/Na^2). \tag{16}$$

N and a retain the same meaning as in Eq. (4). The current given by Eq. (15) differs slightly in structure from expression (4) since in the latter the diffusion term has been neglected. The time-dependent current is computed by Laplace inversion of $I(p)$, using a numerical evaluation of the complex contour integration. Let us now apply Eqs. (15) and (16) to the field-dependent transit experimental data.[30]

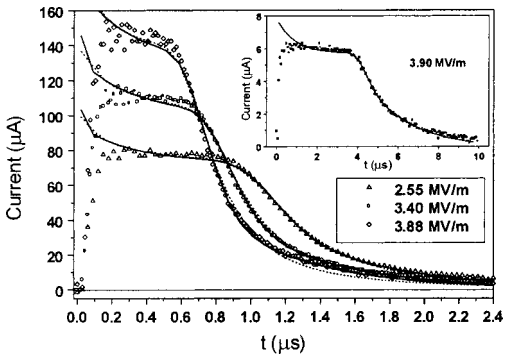

FIG. 3. The transit signal for HAT6 in the liquid-crystalline phase in a 10-μm cell, at temperature $T=353$ K, fitted to Noolandi's single-trap model (solid lines).

V. APPLICATION TO HAT6

In the liquid-crystalline phase, the photocurrent exhibits well-defined transits, which, however, do exhibit some dispersion. Similar dispersions were previously observed in various other liquid-crystalline compounds such as HAT5, HAT5 dimers, and HHTT.[36] Good fits to the transit curves were obtained using Monte Carlo simulations with various trap distribution models.[18] Surprisingly, our data for HAT6 can be explained using single-trap and detrap models as shown in Fig. 3. Throughout the LC phase the transients can be fitted by the same model and the small changes in the mobility values can be accounted for using slightly different trap and release parameters. As pointed out previously, we emphasize that the mobility is essentially independent of temperature and so is the shape of the transient curves. We have therefore focused on one temperature (80 °C) only, and concentrate our modeling on the field dependence of the phototransits. The extracted trapping and release rates w and r are shown in Table I for two different values of the assumed base mobility μ_0. We have chosen to fit the data for two values of the base mobility μ_0. The value $\mu_0=10^{-2}$ cm^2 V^{-1} s^{-1} was chosen because it is close to the estimated upper limit for triphenylene,[37] and the value $\mu_0=10^{-3}$ cm^2 V^{-1} s^{-1} because it is between the upper limit and the trap-limited effective mobility $\mu_{\rm eff}\approx 10^{-4}$ cm^2 V^{-1} s^{-1}, as extracted from the apparent transit times τ of the TOF curves by the relation $\mu_{\rm eff}=L/(F\tau)$. The one-trap model fits all the data perfectly well in both cases. However, we note that both trap and release rates apparently scale linearly with electric field. If the field dependence is introduced explicitly, the delay function can be rewritten as

$$D(p)=D_0/\{1+w^{(0)}/[p/(eFa/2kT)+r^{(0)}]\}, \tag{17}$$

i.e., in such a way that now both $w^{(0)}$ and $r^{(0)}$ are constants, as in the usual trapping models. The electric-field dependence now appears as a scaling factor in the Laplace variable p.

TABLE I. HAT6 trapping and release rates extracted from the fit to the data.

	$\mu_0=10^{-2}$ cm^{2}V^{-1} s^{-1}		$\mu_0=10^{-3}$ cm^{2}V^{-1} s^{-1}	
V	w_1 (Hz)	r_1 (Hz)	w_1 (Hz)	r_1 (Hz)
5	0.497×10^7	0.207×10^6	0.240×10^6	0.160×10^6
10	1.070×10^7	0.447×10^6	0.482×10^6	0.279×10^6
15	1.722×10^7	0.711×10^6	0.673×10^6	0.442×10^6
20	2.306×10^7	0.959×10^6	0.894×10^6	0.593×10^6
25	2.981×10^7	1.239×10^6	1.100×10^6	0.748×10^6

The scaled trap and release rates are shown in Fig. 4, and, as expected, they are almost constant. The implication of Eq. (17) is that the field will scale with the diffusivity such that $D(t)$ becomes $D(eFat/2kT)$. The scaling effectively means that in the presence of the field the particle takes less time to reach the equilibrium diffusivity $D_0/\{1+\langle w^{(0)}/r^{(0)}\rangle\}$. This result is rigorously derivable in the framework of one-dimensional transport theories as shown in Refs. 20 and 23. We have also verified it by solving exactly a model of one trap in a regular periodic lattice. We find that the exact solution obeys reasonably well (though not exactly) the empirical scaling behavior, which we derived in this paper by using the Noolandi model. Note that even in higher dimensions, the drift should accelerate the relaxation function, but in dimensions higher than one, the influence of the drift acts only along one direction, whereas carrier diffusion is in all directions. Hence the drift contribution to the relaxation is small and difficult to see experimentally. In a one-dimensional random walk, however, the carrier can only hop to the right or the left and the number of new sites visited in a time t changes drastically from "$t^{1/2}$" to "$eFt/2kT$" when the field is applied. The effect on the relaxation to equilibrium is very pronounced as shown by the empirical fit to the trap parameters. This is a truly remarkable result, because the assumption made in fitting the data was that the trap and release rates should not be field dependent. The theories of Alexander *et al.* and those of Ref. 23 were not included or assumed.

It should be noted that the dispersion observed in the tail of the transit curves is due to the spread of the carrier packet occurring at short times. In the case of HAT6, the diffusivity decays to the steady-state value within the first few microseconds, but this initial transient, predicted by Eq. (15), is not resolved by the experimental data. The dispersion imparted at the beginning is recovered later, at the collecting electrode. As the field increases, the equilibration becomes faster and correspondingly the dispersion becomes smaller, leading to a sharper tail in the transits.

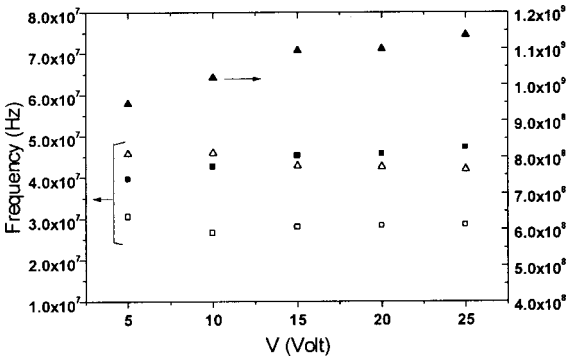

FIG. 4. Plots of the trap and release rates scaled with eFa/kT. The squares correspond to $r^{(0)}$ and the triangles to $w^{(0)}$, while the open symbols are related to $\mu_0=10^{-3}$ cm^{2}V^{-1} s^{-1} and the filled symbols to $\mu_0=10^{-2}$ cm^{2}V^{-1} s^{-1}.

It is possible to make the following observations regarding the values obtained for the fits:

(i) The release rate $r^{(0)}\sim10^7$ Hz is consistent with the low-frequency liquidlike fluctuations ranging in the interval 10^5-10^9 Hz. In the working hypothesis that the traps are due to order fluctuations within each molecular column, the detrapping rate matches the self-repairing frequency of these defects.

(ii) As expected, the release rate is not sensitive to the choice of the initial mobility μ_0.

(iii) The definition of the trap rate $w^{(0)}$ includes the concentration of traps. It should be properly rewritten as $w^{(0)}=t^{(0)}x$, with x the trap concentration, or probability of being trapped at each molecular site. The trap frequency $t^{(0)}$ can be set equal to the intermolecular hop rate W, because this is the rate at which the carrier encounters new potential traps. In this case it is possible to extract a value for the trap probability $x\sim5\times10^{-4}$ relative to the mobility $\mu_0=10^{-2}$ cm^2 V^{-1} s^{-1}, and a value $x\sim1\times10^{-3}$ relative to the mobility $\mu_0=10^{-3}$ cm^2 V^{-1} s^{-1}. The two values are consistent and imply that approximately every 1000 hops the carriers encounter a difficult obstacle and are delayed by the trap time. In a cell of 10-μm width, this implies that a carrier gets trapped $\sim$30 times along its journey to the counterelectrode.

Donovan *et al.* fitted the photocurrent transient in the crystalline phase with a similar one-trap model.[21] They have argued that the photocurrent transients in the Cr phase appear to reach a steady-state value[38] when the carriers have crossed roughly $\frac{1}{10}$ of the cell width. At that point in time and space, the photocurrent, though an order-of-magnitude smaller, still represents a sizeable fraction of the peak value. The exponential function used in Ref. 18 fits the decay rather well. The trap and release rates deduced in the crystalline phase at a field of 2.5×10^4 V/cm are $w=4.5\times10^5$ and $r=4.0\times10^4$ Hz, respectively. The extracted trap-free mobility is $\mu_0=2.6\times10^{-3}$ cm^2 V^{-1} s^{-1}. In the Col_h phase we find, at the same value of the field, a trap rate $w=1.0\times10^6$ Hz, and a release rate $r=7.5\times10^5$ Hz for the trap-free mobility of

TABLE II. Parameters used to fit the data of the mixed system HAT11-PTP9 to the two-trap model.

L (μm)	F (MV m^{-1})	w_1 (Hz)	r_1 (Hz)	w_2 (Hz)	r_2 (Hz)
4.7	2.55	4.384×10^7	4.919×10^7	1.430×10^6	2.350×10^6
4.7	3.40	5.277×10^7	5.415×10^7	1.624×10^6	2.374×10^6
4.7	3.88	4.726×10^7	5.512×10^7	1.637×10^6	2.388×10^6

$\mu_0=1.0\times10^3$ cm^2 V^{-1} s^{-1} (Table I). If the apparent steady state observed by these authors is a true steady state, then one should expect to see a transient in the Cr phase as well. Note that the final drift velocities in the two phases are apparently very similar. The trap and release rates can be used to extract the trap-limited carrier velocity in the crystalline phase, which is then given by $\nu=\mu_0 Fr/(r+w)=5.3$ cm/s. Similarly for the mesophase we obtain $\nu=10$ cm/s. In the Cr-phase data of Ref. 18 the cell width is 20 μm, hence the transit to the boundary should normally occur at about 400 μs after the light pulse. However, the transients were observed for only the first 10 μs after the light pulse, and during this time the carriers have traveled only about 3.5 μm of the sample. The similarity between the values found for the trap and release rates in the two phases is intriguing. It suggests that the mechanism involved in the trapping process is essentially the same. This could be associated in both cases with columnar defects: in one case the defect is frozen and static and due to polycrystallinity, and in the other case, the same or similar defect is dynamic and self-repairing.

VI. APPLICATION TO THE BINARY CPI COMPOUND HAT11-PTP9

This model has also been applied to interpret the TOF data for the 1:1 mixed system HAT11-PTP9. The molecules and the ideal columnar assembly are represented in Fig. 1. This compound shows remarkable properties and generally gives a structurally more ordered system, with substantially increased carrier mobility as compared to single-component HATn systems.[16] As discussed in detail in Ref. 12 the two molecules self-assemble in alternating *AB* stacks, and these stacks then self-organize into a hexagonal columnar array (Fig. 1). For this compound the field dependence was analyzed at the fixed temperature of 120 °C, which is representative of the transient behavior in the whole LC range. The TOF transients show an apparently flat plateau, after which there is a strong dispersive decay that cannot be understood on the basis of the single-trap model proposed for HAT6. The time scale excludes the possibility of ionic transport, since the movement of ions would be too slow, therefore the long tail implies disorder. Logically we should expect three types of disorder in this material. In addition to the two types of disorder described for the single-component HATn system, there is also disorder due to the occasional *AA* or *BB* defect within the *AB* stacked columns.

In order to understand the TOF-photoconductivity transits, it is crucial to know how frequently such symmetry breaking occurs. If they occur on a short length scale (10 nm) then the disorder can be included within the definition of the base diffusivity D_0 [Eq. (6)], and its effect will not be observable on the present time scale. On the other hand if they occur on a length scale of microns, then they could well be the reason for the observed dispersion. Unfortunately estimates of the correlation length for such a system cannot be obtained from one-dimensional (1D) self-assembling thermodynamics,[39] since, in reality, the system is not strictly 1D. There is also the question of how much of an obstacle such a defect would represent in terms of a trap and release time. From quantum-mechanical semiempirical computations we have estimated that the HOMO levels of the two molecules differ by ~0.2 eV (HAT1, 8.45 eV; PTP1, 8.26 eV).[40] In the temperature range of interest this would apparently not cause a serious obstacle to the mobility. Since our information at the moment is not adequate to make firm predictions on the nature and magnitude of the trap distribution beyond the remarks made above, we have therefore, at this stage, taken an empirical approach to modeling the data. We started by fitting the data using the Noolandi model (with one, two, and three traps), then we tried the Scher-Lax distribution, and finally, since neither gave completely satisfactory agreement with the measurements, we also attempted an inhomogeneous interfacial trapping model.

To fit the TOF transits with Noolandi's model, at least two different types of traps are needed. The results are summarized in Table II and typical fits are shown in Fig. 5. In this case the base mobility was assumed to be $\mu_0=3\times10^{-2}$ cm^2 V^{-1} s^{-1} (higher than in HAT6). It should be noted that this value is slightly larger than the estimated upper limit of 0.025 cm^2 V^{-1} s^{-1} along triphenylene cores, but the value employed was the lowest value allowed in order to obtain good fits.[37,41] The lower value $\mu_0=2\times10^{-2}$ cm^2 V^{-1} s^{-1}, for example, would imply a longer

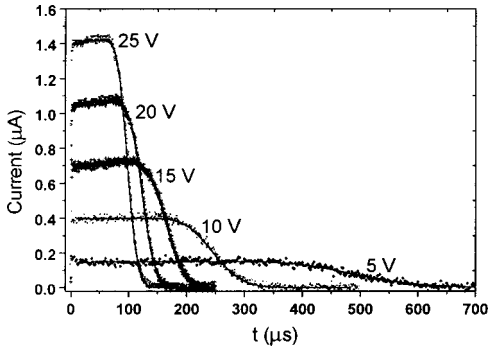

FIG. 5. The phototransit signal in the mixture HAT11/PTP9 at $T=400$ K in a 4.7-μm cell. The solid lines are the fits to Noolandi's two-trap model and the broken lines are the fits to the Scher-Lax distribution model. The inset shows the fits to the data for the 25-μm cell. The assumed base mobility in the fits is $\mu_0=3\times10^{-2}$ cm^{2}V^{-1} s^{-1}.

TABLE III. Parameters used in the Scher-Lax distribution model for the mixed system HAT11-PTP9.

F (MV m^{-1})	n	ν_0 (Hz)	$\nu_{\min}$ (Hz)	$\nu_{\max}$ (Hz)	$R_{\max}$ (nm)	$R_{\min}$ (nm)	α (nm^{-1})
2.55	2.508×10^3	4.153×10^{10}	4.620×10^5	2.798×10^8	1.140	0.50	5
3.40	2.573×10^3	5.653×10^{10}	3.294×10^5	3.808×10^8	1.205	0.50	5
3.88	2.475×10^3	4.962×10^{10}	2.747×10^5	3.343×10^8	1.210	0.50	5

transit time than the one observed, making it impossible to fit the data. One question that may arise is whether or not the assumption that the carriers really cross the entire cell width or that the field is uniform is valid. Both hypotheses were apparently confirmed using measurements on cells of 25.6-μm width (Fig. 5, inset). In this case the transit time scales perfectly with the one obtained for the cell of 4.7 μm, shown in Fig. 5. This rules out the suggestion that what is observed is actually a pseudotransit due to domain formation or a space-charge effect.

The fits to the two-trap model, shown in Fig. 5, are reasonably good. The long dispersive tail is well reproduced; the agreement is, however, not very convincing in the short-time limit, although it should be said that in this region, there is a large instrumental uncertainty, hence the data are difficult to interpret. The model also seems to fail in reproducing the shape of the transit knee. We discovered that the introduction of a third trap does not produce any improvement. We then tried to model the data using the *R*-hopping Scher-Lax distribution function of delay times given by[42]

$$D(p)=D_0/\left(1+\sum_i \{\nu_0\exp(-2\alpha R_i)/[p+\nu_0\exp(-2\alpha R_i)]\}\right), \tag{18}$$

which can be written as a continuous distribution function,

$$\Sigma(p)=n\int_{R_{\min}}^{R_{\max}}\frac{\nu_0 e^{-2\alpha R}}{p+\nu_0 e^{-2\alpha R}}dR=\frac{n}{2\alpha}\ln\left[\frac{p+\nu_0 e^{-2\alpha R_{\min}}}{p+\nu_0 e^{-2\alpha R_{\max}}}\right] \tag{19}$$

with n the trap linear density. This function assumes that trapping and release are symmetric processes caused by capture of charges from configurations that are not in the immediate transport channel. The results of the fits are shown in Fig. 5, where it can be seen that the distribution of traps does not make any significant improvement to the two-trap model. After having defined $\nu_{\min}=\nu_0\exp(-2\alpha R_{\max})$ and $\nu_{\max}=\nu_0\exp(-2\alpha R_{\min})$, the quantities n, $\nu_{\min}$, and $\nu_{\max}$ were treated as independent variables in the fitting procedure. The parameter α was set such that $2\alpha=10$ nm^{-1}. The values obtained from the fit are shown in Table III.

In contradiction to HAT6, the fit parameters in the mixed system do not show a dependence with the applied field. This would, in principle, seriously question the validity of the trapping model for the binary compounds. The ''logic'' used for the one-dimensional field-dependent kinetic should be true here as well and perhaps even more so because there is experimental evidence of a more pronounced one-dimensional columnar stability. One difference between the two systems is that the mobility in HAT11-PTP9 is much higher than in HAT6. The observed transit times in the mixed system are compatible with the upper limit of the mobility $\mu_0=3\times10^{-2}$ cm^2 V^{-1} s^{-1}. Indeed, even though the mobility in the mixed system is time dependent, the effect of the trapping on its long-time value is apparently small. In HAT6 the highest experimentally observable mobility is one to two orders-of-magnitude smaller than the effective long-time value. In the mixed system, short- (0.2 μs) and long-time mobility only appear to differ by a factor of 3. This implies that the carriers do not experience any significant trap delay during the time of flight—a remarkable conclusion given the fact that one would expect a mixed system to have more disorder than a single-component system (due to the inherent difficulty involved in preparing *AB* mixtures with exact 1:1 stoichiometry).

Up to now we have assumed that the traps are homogeneously distributed throughout the cell. The initial plateau in the transient photocurrent data suggests that carriers are moving without serious delays for a while, until they reach a trap-rich region, which emanates from the collecting electrode. The data could therefore be interpreted in terms of disorder that is not uniform: trapping delay is more likely to occur near the boundaries than in the bulk. This does not contradict the model used for HAT6 since in the latter case, the bulk trapping delay is much longer, and the interface does not play an important role. To accommodate the hypothesis of boundary trapping, we have compared the data using a model function of the form

$$I(t)=I_0\{1-\exp(-t_0/t)^{\beta}\}. \tag{20}$$

This says that t_0 is of the order of the time taken for carriers to reach the trap-rich region and β is an exponent that is a measure of the sharpness of the transit region. If t_0 is much smaller than the transit time, the diffusivity exhibits the usual power-law decay characteristic of uniform trapping.

The typical fit is shown in Fig. 6, and is clearly better than the two other models since it manages to reproduce the flat plateau, the sharp knee, and the stretched, dispersive tail although the tail is not perfectly fitted by the functional form of Eq. (20). Importantly, the empirical form (20) also has the scaling behavior with cell thickness observed experimentally. The problem now is that this functional form does not agree with the assumption that the decay of the photocurrent is independent of the history of the carrier motion. In fact, Eq. (20) says that a thin cell exhibits a sharper decay than a thick cell. In other words this model implies that the effective width of the trap-rich region increases with cell thickness. This conclusion, however, contradicts the original assump-

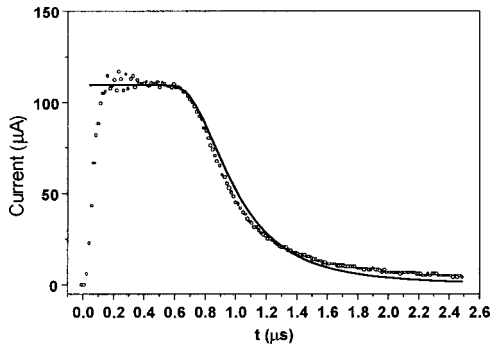

FIG. 6. TOF signal for the mixed system fitted using the boundary trap model.

tion and implies that the trapping must be at least to some extent bulk limited. We note therefore that although the empirical function fits the data better than the other models, it is not easy to justify the physical situation that it implies.

VII. CONCLUSIONS

In our last summary published in Ref. 6 we pointed out that the differences in the 1D to 3D kinetics appear in the trap-controlled photocurrent decay and field dependencies. Photocurrent decays in the Col_h phase, where there are high concentrations of deep traps, are particularly good examples of one-dimensional kinetics. This was also demonstrated in Ref. 6 using the field-dependent data gathered in the crystalline phase. We also argued that the mobility in one dimension should exhibit anomalies as a function of field because self-averaging implies visiting a sufficiently large number of representative rate-limiting new configurations. This takes less time in a high field. In this paper we have now demonstrated that for cells of 4 μm in width, the diffusivity is trap controlled. The average distance between traps is found to be of the order of 1000 molecules (0.3 μm). The TOF transits for the Col_h phase of HAT6 were successfully reproduced using the surprisingly simple model of a single type of shallow trap, randomly distributed within the cell. We associate this kind of trapping with the random, liquidlike fluctuations occurring in the columnar mesophase of HAT6 [Fig. 1(a)].

Unfortunately we have not been able to produce a completely satisfactory fit to the data obtained from the 1:1 binary CPI compound HAT11-PTP9 using the same model. A concern is that in this case the time-dependent (short-time) diffusivity does not appear to depend on the applied electric field. However there are good reasons why this may be so: the trapping kinetics in the experimental time domain cause only a relatively small change to the diffusivity and any field dependence is probably too difficult to extract with present experimental accuracy. The Scher-Lax structural delay-time model also gives excellent fits to the long-time tail but it is again not entirely consistent with the short-time plateau of the photocurrent. For fitting purposes, the data can be better represented using an empirical function that mimics an inhomogeneous interfacial trapping model. This model, however, also implies that the width of the trap-rich region increases with cell width (not easy to justify). On the other hand with homogeneous trap models that it is difficult to get a plateau and a long-time tail. It is perhaps not surprising that a mixed material exhibits more complexity in carrier generation, trapping scenarios, and trap distributions. The initial shape of the free charge packet may be more complex than the one assumed in the present derivation. The models we have used in this paper are well established and represent a good starting point on which further work will build.

ACKNOWLEDGMENTS

T.K. and K.J.D. acknowledge the support of the Leverhulme Trust, Grant No. F/476/AB, for funding the experimental work. B.M. would like to thank the Leverhulme Trust for a fellowship and Dr. Harvey Sher for his valuable comments and suggestions.

*Email address: soms@chem.leeds.ac.uk; URL: http// www.chem.leeds.ac.uk/SOMS/home.htm

†Corresponding author.

‡Current address: Department of Physics, Imperial College of Science, Technology and Medicine, Prince Consort Road, London SW7 2BZ, United Kingdom.

[1] S. Chandraekhar, *Liquid Crystals* (Cambridge University, Cambridge, England, 1980).

[2] N. Boden, R. J. Bushby, J. Clements, M. V. Jesudason, P. F. Knowles, and G. Williams, Chem. Phys. Lett. **152**, 94 (1988).

[3] D. Adam, F. Closs, T. Frey, D. Funhoff, D. Haarer, H. Ringsdorf, P. Schuhmacher, and K. Siemensmeyer, Phys. Rev. Lett. **70**, 457 (1993).

[4] D. Adam, P. Schuhmacher, J. Simmerer, L. Haussling, K. Siemensmeyer, K. H. Etzbach, H. Ringsdorf, and D. Haarer, Nature (London) **371**, 141 (1994).

[5] N. Boden, R. J. Bushby, J. Clemens, B. Movaghar, K. Donovan, and T. Kreouzis, Phys. Rev. B **52**, 13 274 (1995).

[6] N. Boden, R. J. Bushby, J. Clemens, B. Movaghar, K. Donovan, and T. Kreouzis, Phys. Rev. B **58**, 3063 (1998).

[7] B. Movaghar, J. Mol. Electron. **3**, 183 (1988).

[8] N. Boden, R. J. Bushby, and A. N. Cammidge, J. Chem. Phys. **98**, 5920 (1993).

[9] J. M. Warman, M. P. Dehaas, K. J. Smit, M. N. Paddonrow, and J. F. Vanderpol, Mol. Cryst. Liq. Cryst. **183**, 375 (1990).

[10] X. Shen, R. Y. Dong, N. Boden, R. J. Bushby, P. S. Martin, and A. Wood, J. Chem. Phys. **108**, 4324 (1998); R. Y. Dong, D. Goldfarb, M. E. Moseley, Z. Luz, and H. Zimmermann, J. Phys. Chem. **88**, 3148 (1984).

[11] A. M. Levelut, J. Phys. (France) Lett. **40**, L81 (1979).

[12] E. O. Arikainen, N. Boden, R. J. Bushby, O. R. Lozman, J. G. Vinter, and A. Wood, Angew. Chem. Int. Ed. Engl. **39**, 2333 (2000).

[13] N. Boden, R. J. Bushby, G. Headdock, O. R. Lozman, and A. Wood, Liq. Cryst. **28**, 139 (2001).

[14] N. Boden, R. J. Bushby, G. Headdock, O. R. Lozman, A. Wood, E. O. Arikanien, A. P. McNeill, K. J. Donovan, T. Kreouzis, Z. Lu, and Q. Liu, Report No. UKP36278W, 2000 (unpublished).

[15] O. R. Lozman, R. J. Bushby, G. Cooke, and Z. Lu, J. Am. Chem. Soc. **123**, 7915 (2001). http://dx.doi.org/10.1021/ja003443b.

[16] O. R. Lozman and R. J. Bushby, J. Chem. Soc., Perkin Trans. 2 **9**, 1446 (2001).
[17] T. Kreouzis, K. Scott, K. J. Donovan, N. Boden, R. J. Bushby, O. R. Lozman, and Q. Liu, Chem. Phys. **262**, 489 (2000).
[18] A. M. van de Craats *et al.*, J. Phys. Chem. B **102**, 9625 (1998).
[19] D. Markovitsi, F. Rigaut, M. Mouallem, and J. Malthete, Chem. Phys. Lett. **135**, 236 (1987).
[20] B. Movaghar, D. Wurtz, and B. Pohlmann, Z. Phys. B: Condens. Matter **66**, 523 (1987).
[21] K. J. Donovan, T. Kreousis, N. Boden, and J. Clements, J. Appl. Phys. **109**, 10 400 (1998).
[22] B. Movaghar, B. Pohlmann, and D. Wurtz, Phys. Rev. A **29**, 1568 (1984).
[23] S. Alexander, J. Bernasconi, W. R. Schneider, and R. Orbach, in *Physics in One Dimension*, edited by J. Bernasconi and T. Schneider, Springer Series in Solid State Science (Springer, Berlin, 1981), Vol. 23, p. 277.
[24] D. Markovitsi, I. Lecuyer, P. Lianos, and J. Malthete, J. Chem. Soc., Faraday Trans. **87**, 1785 (1991); D. Markovitsi, S. Marguet, L. K. Gallos, H. Sigal, P. Millie, P. Argyrakis, H. Ringsdorf, and S. Kumar, Chem. Phys. Lett. **306**, 163 (1999).
[25] R. Haberkorn and M. E. Beyerle, Chem. Phys. Lett. **23**, 128 (1973).
[26] R. Bilke, A. Schreiber, I. Bleyl, D. Haarer, and D. Adam, J. Appl. Phys. **87**, 3872 (2000).
[27] T. Kreouzis and K. Donovan (private communication).
[28] M. A. Palenberg, R. J. Silbey, M. Malagoli, and J. L. Bredas, J. Chem. Phys. **112**, 1785 (2000).
[29] J. Noolandi, Phys. Rev. B **16**, 4466 (1977).
[30] The details of the TOF experiment results are given in Ref. 35.
[31] H. Scher and E. W. Montroll, Phys. Rev. B **12**, 2455 (1975).
[32] B. Movaghar, M. Grunewald, B. Pohlmann, D. Wurtz, and W. Schirmacher, J. Stat. Phys. **30**, 315 (1983).
[33] T. Kreouzis, K. J. Donovan, N. Boden, R. J. Bushby, O. R. Lozman, and Q. Liu, J. Chem. Phys. **114**, 1797 (2001).
[34] T. Holstein, Ann. Phys. (N.Y.) **8**, 325 (1959).
[35] H. Sumi, Solid State Commun. **29**, 495 (1979).
[36] D. Adam *et al.*, Phys. Rev. Lett. **70**, 457 (1993); D. Adam, W. Romhidt, and D. Haarer, in *Proceedings of the International Workshop on Advanced Materials*, edited by T. Kodama (ONRI International Workshop on Advanced Materials, Osaka, 1995), p. 100; I. Bleyl *et al.*, Philos. Mag. B **79**(3), 463 (1998).
[37] A. M. van de Craats and J. M. Warman, Adv. Mater. Opt. Electron. **13**, 130 (2001).
[38] See Fig. 6 in Ref. 18, and the discussion therein.
[39] J. R. Henderson, J. Chem. Phys. **113**, 5965 (2000).
[40] Calculated at PM3 level on structures minimized to accuracy of ± 0.01 kJ mol^{-1}. The computer code HYPERCHEM, Ver 5.1, Hypercube Inc., was used to perform the calculations on a standard IBM compatible personal computer.
[41] The values quoted in Ref. 37 refer to the triphenylene core alone. Since the conjugated π core of HAT*n* is larger than that of triphenylene we feel justified in using the slightly higher value of 3×10^{-2} cm^{2}V s^{-1} as the upper limit for the base mobility.
[42] H. Scher and M. Lax, Phys. Rev. B **7**, 4491 (1973); **7**, 4502 (1973).